

CASE REPORT

ADVANCED

CLINICAL CASE

What Is Hidden Behind Inferior Negative T Waves



Multiple Cardiac Glomangiomas

Vincenzo Castiglione, MD,^a Alberto Aimo, MD,^a Bruno Murzi, MD,^b Angela Pucci, MD, PhD,^c Giovanni Donato Aquaro, MD,^b Andrea Barison, MD, PhD,^{a,b} Alberto Clemente, MD,^b Valentina Spini, MD,^b Giovanni Benedetti, MD,^b Michele Emdin, MD, PhD^{a,b}

ABSTRACT

Negative T waves in the inferior leads in an asymptomatic 17-year-old female patient prompted a diagnostic evaluation disclosing the presence of multiple cardiac glomangiomas. The combination of different imaging modalities (echocardiography, magnetic resonance, and positron emission tomography/computed tomography) and myocardial biopsy was crucial to establishing the correct diagnosis. (**Level of Difficulty: Advanced.**) (J Am Coll Cardiol Case Rep 2019;1:657-62) © 2019 The Authors. Published by Elsevier on behalf of the American College of Cardiology Foundation. This is an open access article under the CC BY-NC-ND license (<http://creativecommons.org/licenses/by-nc-nd/4.0/>).

HISTORY OF PRESENTATION

An asymptomatic 17-year-old female patient with a negative clinical history underwent a pre-participation screening for noncompetitive sports activity.

MEDICAL HISTORY

A 12-lead electrocardiogram showed negative T waves in the inferior leads (**Figure 1**). A transthoracic echocardiogram indicated the presence of cardiac masses in both ventricles (**Figure 2**, **Video 1**).

LEARNING OBJECTIVES

- Nonspecific T-wave changes may underlie the presence of large cardiac masses.
- CMR findings suggestive of malignancy, such as infiltration of myocardial tissue, encasement of coronary arteries, and heterogeneous tissue signal, may correspond to benign lesions.
- Whole-body PET/CT scan and histological examination are essential to assess the nature of a cardiac mass.
- Multiple angiomatous-like cardiac mass diagnostic evaluation should consider cardiac glomus tumors in the differential etiological diagnosis.

DIFFERENTIAL DIAGNOSIS

Cardiac magnetic resonance (CMR) imaging confirmed the presence of 4 transmural masses. The largest one (73 × 22 × 64 mm) encased the right coronary artery, the anterior wall of the right ventricle, and the right atrium (**Figure 3A**); another one surrounded the left anterior descending artery and the anterior wall of the left ventricle (**Figure 3B**); a third mass involved the basal lateral left ventricular wall within the circumflex artery territory (**Figure 3C**), and a fourth, smaller lesion was located in the basal diaphragmatic wall, vascularized by the left posterior descending artery (**Figure 3D**). On T1- and T2-weighted images, the lesion involving the right ventricle was much more

From the ^aInstitute of Life Sciences, Scuola Superiore Sant'Anna, Pisa, Italy; ^bFondazione Toscana Gabriele Monasterio, Massa and Pisa, Italy; and the ^cDepartment of Histopathology, University Hospital, Pisa, Italy. The authors have reported that they have no relationships relevant to the contents of this paper to disclose.

Informed consent was obtained for this case.

Manuscript received September 17, 2019; revised manuscript received October 21, 2019, accepted October 22, 2019.

**ABBREVIATIONS
AND ACRONYMS****CMR** = cardiac magnetic resonance**CT** = computed tomography**PET** = positron emission tomography

hyperintense than the ones located in the left ventricle, suggesting more interstitial edema. All masses were highly perfused, as shown by the rapid and homogeneous early enhancement; delayed enhancement was diffuse and inhomogeneous and more evident in the right ventricular mass. Finally, a slight circumferential pericardial effusion was present (8 mm at the end-diastole) (**Figure 4**, **Videos 2** and **3**). On cardiac computed tomography (CT) scans, the lesions exhibited early post-contrast enhancement, a density similar to the aorta during the whole cardiac cycle, and ectatic veins (i.e., a pattern typical of angiomatous lesions or arteriovenous malformations). The very high degree of vascularization was confirmed by using coronary angiography (**Figure 5**, **Videos 4** and **5**).

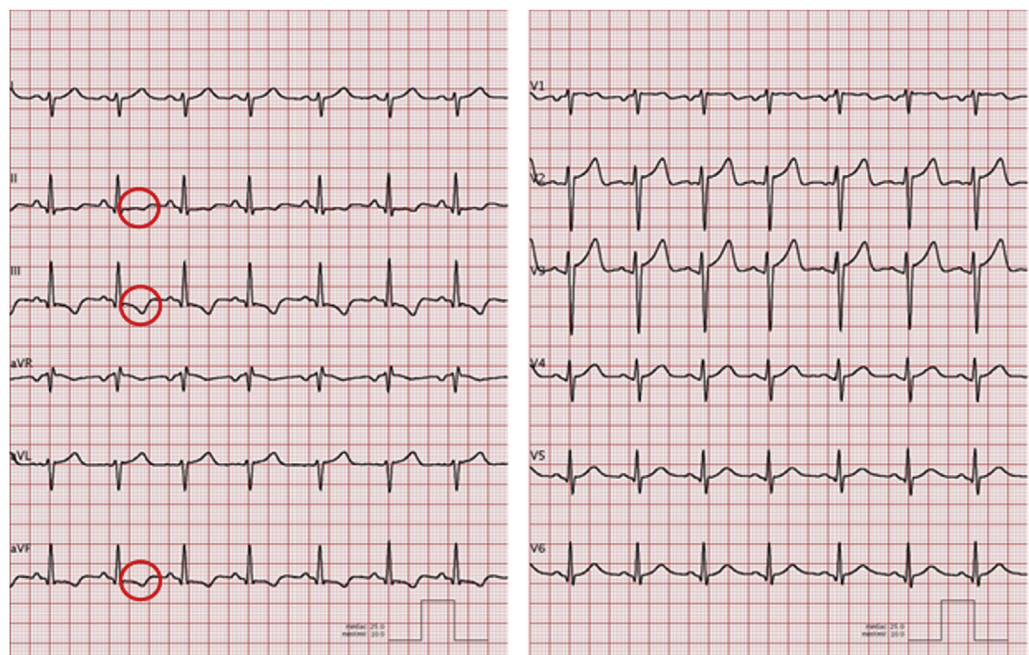
INVESTIGATIONS

To assess the nature of the masses, the patient underwent a positron emission tomography (PET)/CT scan, which did not show pathological ^{18}F -fluorodeoxyglucose uptake in the heart or other tissues (**Supplemental Figure 1**). Furthermore, biopsies of the right ventricular lesion, raising the greatest suspicion of malignancy at CMR, and pericardial fluid sampling

were performed through an inferior mini-sternotomy. The histological examination of 5 samples confirmed that the lesions extended from the epicardial surface to the nearby healthy myocardium, with no clear separation. The masses consisted of nests of rounded medium-sized cells with regular ovoid nuclei, lightly eosinophilic cytoplasm, and well-demarcated borders. Cells aggregated around dilated vessels of various size and did not exhibit necrosis or any significant cytological abnormality or mitotic activity (MIB-1 proliferation index $\leq 1\%$) (**Figure 6**). At immunohistochemistry, cells displayed strong reactivity for markers of smooth muscle cells (alpha smooth muscle actin and caldesmon), and immunostaining for S100, pan cytokeratin AE1/AE3, calretinin, synaptophysin, and chromogranin was negative. These features allowed a final diagnose of a cardiac glomangioma. Rare reactive mesothelial cells were retrieved from the pericardial fluid.

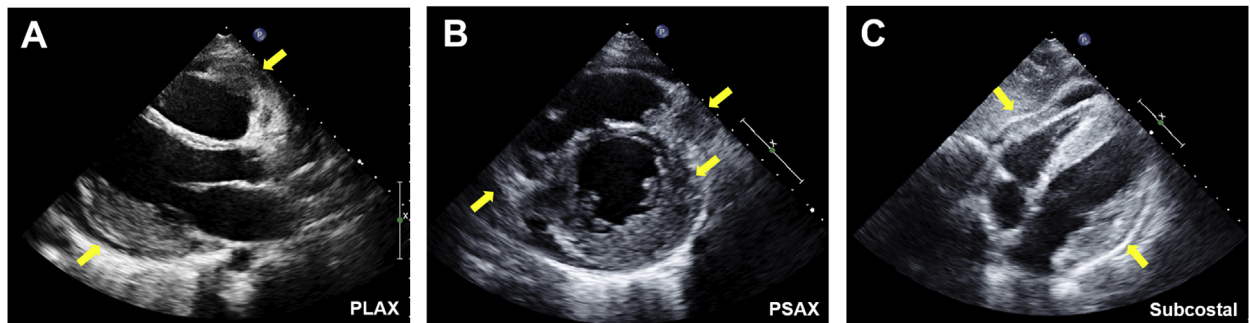
MANAGEMENT

Because the cardiac lesions were unresectable and did not affect cardiac hemodynamic parameters, the patient was discharged on propranolol 20 mg three times daily.

FIGURE 1 Electrocardiogram

Electrocardiogram displaying negative T waves in inferior leads.

FIGURE 2 Transthoracic Echocardiogram



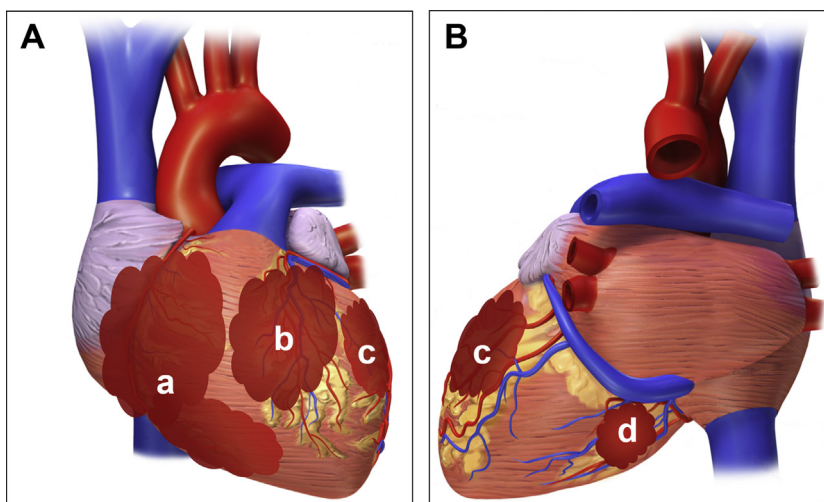
Transthoracic echocardiogram showing multiple cardiac masses: parasternal long axis view (A), parasternal short axis view (B), subcostal view (C). See Video 1. PLAX = parasternal long axis; PSAX = parasternal short axis.

DISCUSSION

Glomus tumors are rare mesenchymal neoplasms representing <2% of soft tissue tumors. They usually develop in the subungual regions or the deep dermis of the palm, wrist, forearm, and foot, although rare visceral localization has also been described. Glomus tumors usually present as well-circumscribed lesions composed of small vessels surrounded by cuffs of smooth muscle cells. They arise from smooth muscle cells of glomus bodies, which are specialized arteriovenous anastomoses contributing to temperature regulation in the skin (1). Glomus tumors may be

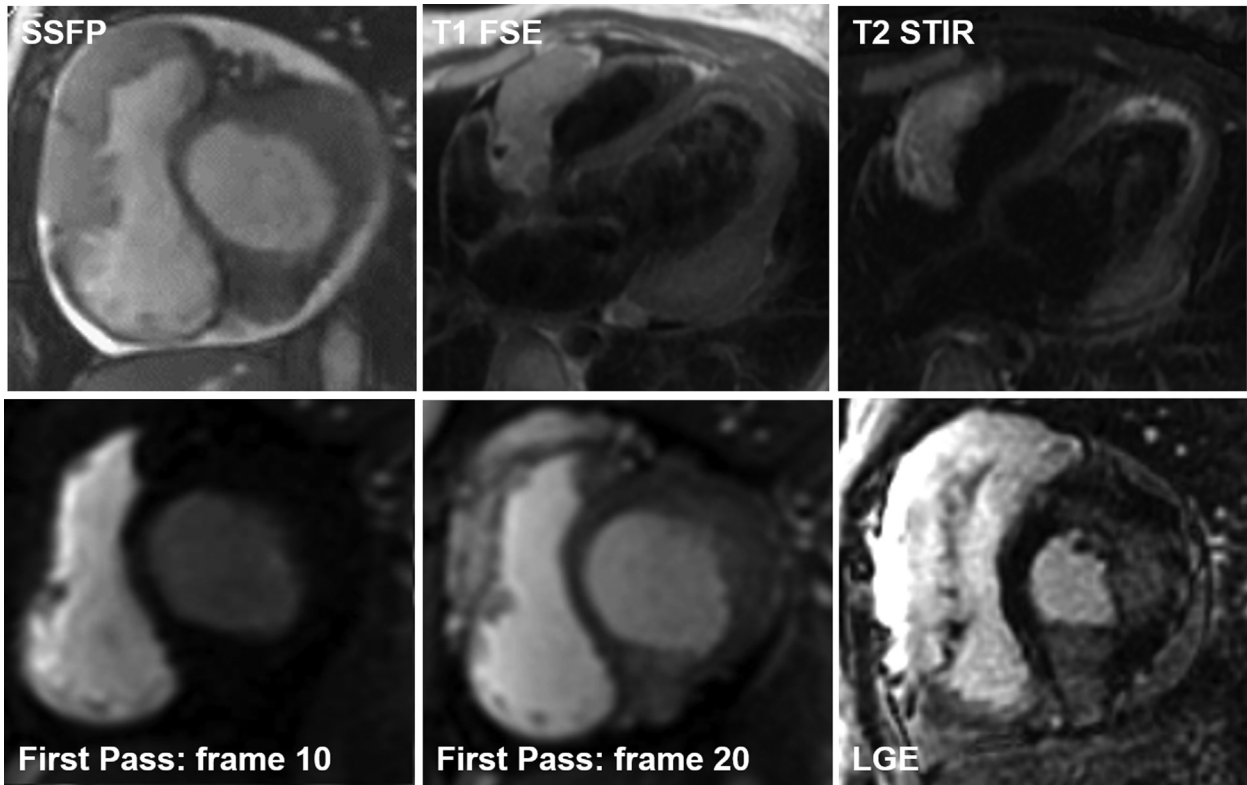
subcategorized as solid glomus tumors (with poor vasculature and a small smooth muscle component; 75%), glomangioma (with a prominent vascular component; 20%), or glomangiomyoma (with both vascular and smooth muscle components; 5%). Nearly 10% of glomus tumors are multiple, often with a positive family history. Familial glomus tumors usually derive from mutations in the *GLMN* gene, encoding for glomulin, a regulator of vessel development (2). Neurofibromatosis has also been associated with the development of these neoplasms (3). About 1% of glomus tumors are malignant (glomangiosarcoma). Histological criteria for malignancy

FIGURE 3 Localization of Cardiac Masses



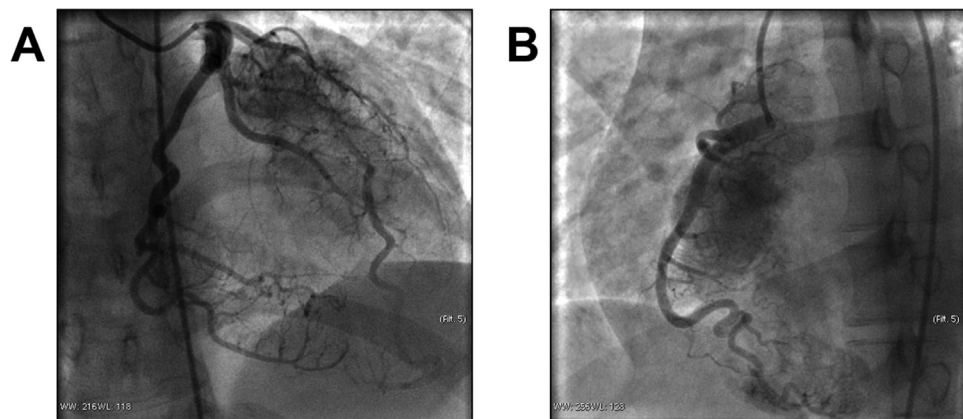
Localization of the 4 cardiac masses (a, b, c, d) on the (A) anterior and (B) posterior view of the heart.

FIGURE 4 Cardiac Magnetic Resonance



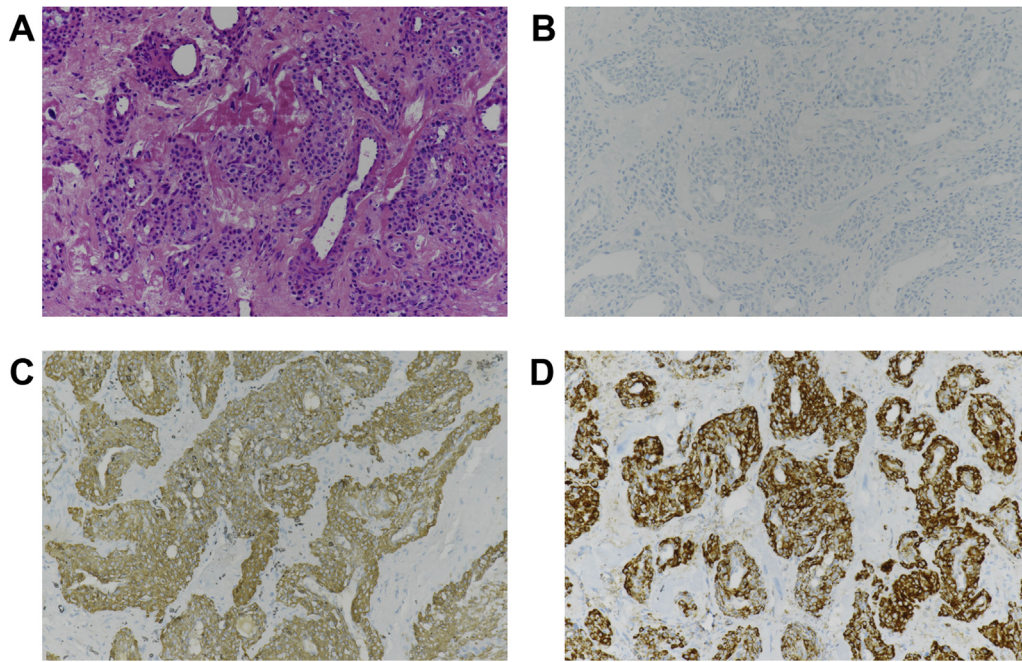
Distribution and tissue signal appearance of the lesions at cardiac magnetic resonance. See [Videos 2 and 3](#). FSE = fast-spin echo; LGE = late gadolinium enhancement; SSFP = steady-state free precession; STIR = short-tau inversion recovery.

FIGURE 5 Coronary Angiography



Coronary angiography views of the (A) left coronary artery and (B) right coronary artery. See [Videos 4 and 5](#).

FIGURE 6 Histology of a Cardiac Benign Glomangioma



Optical microscopy (20× magnification): (A) hematoxylin and eosin stain; (B) low mitotic activity (MIB-1 proliferation index $\leq 1\%$); and (C, D) immunoreactivity for alpha smooth muscle actin and caldesmon, respectively.

include visceral location, size ≥ 2 cm, atypical mitotic figures, and increased proliferation (4).

Glomus tumors must be differentiated from hemangiomas, neuroendocrine tumors, paragangliomas, and smooth muscle tumors. Glomus tumors do not express endothelial markers as with hemangiomas but are immunoreactive with smooth muscle actin and caldesmon. They also do not stain for neuroendocrine markers such as synaptophysin, chromogranin, and S100. The differential diagnosis between glomus tumors and other smooth muscle tumors relies on clinical presentation and specific histological features (1,5).

Only 5 cases of solitary cardiac glomus tumors have been reported so far. In 1975, this diagnosis was made in a 28-year-old woman with heart failure and a large left ventricular mass (6). A cardiac glomangioma was also identified in the right atrium of a 37-year-old woman presenting with dyspnea and palpitations (7) and in the anterolateral left ventricular wall of an asymptomatic 67-year-old man (8). Two cases of malignant glomangioma have been recently described: one attached to the anterior interventricular septum and anterolateral left ventricular wall in a 64-year-old man hospitalized for ischemic stroke

(5), and another adherent to the posterior wall of the left atrium and posterior mitral leaflet in a 31-year old woman presenting with atrial flutter (9).

Differently from all previous cases, our patient had multiple cardiac lesions, which were characterized through various noninvasive imaging modalities and coronary angiography. The original description of negative T waves on the inferior leads was likely associated with the presence of a glomangioma in the inferior wall. Although tissue infiltration and heterogeneous tissue signal at CMR were suggestive of malignancy, PET/CT imaging did not show any pathologic uptake at heart level or metastases. The high degree of vascularization at CT scanning and coronary angiography was compatible with a diagnosis of angioma, arteriovenous malformation, or angiosarcoma. Biopsy of the mass was crucial to establish the final diagnosis, displaying typical morphological and immunohistochemical features and the absence of nuclear atypia or proliferation. The benign diagnosis and the impossibility of surgically resecting the masses prompted conservative therapy with oral propranolol, based on the evidence that this drug has induced regression of neonatal cardiac hemangiomas (10).

FOLLOW-UP

At 1-month follow-up, the patient remained asymptomatic, and the propranolol dose was up-titrated to 40 mg three times daily. At 3 months, a CMR examination showed unchanged mass sizes. Because myocardial ischemia due to a steal mechanism could not be excluded, an exercise echocardiogram was performed at 4 months. This examination revealed slight, nonspecific ST-segment depression in inferior and antero-lateral leads at maximal exercise (125 W, rate-pressure product 26,400) in the absence of regional wall motion abnormalities. A moderate-intensity aerobic physical activity (maximum heart rate 110 beats/min) was then allowed. In the absence of any knowledge regarding disease evolution from previous literature, a follow-up with transthoracic echocardiograms every 6 months was planned.

First-degree relatives (parents and a younger brother) were screened. They exhibited no

clinical, electrocardiographic, or echocardiographic abnormalities.

CONCLUSIONS

Subtle T-wave changes may underlie the presence of large cardiac masses. Even benign lesions can present with CMR findings suggestive of malignancy, such as infiltration of adjacent myocardial tissue, encasement of coronary arteries, and heterogeneous tissue signal. Whole-body PET/CT scan and histological examination are crucial to establish the correct diagnosis.

ACKNOWLEDGMENT The authors thank Emilio Pasanisi, MD, for his contribution to the diagnostic evaluation of this patient.

ADDRESS FOR CORRESPONDENCE: Dr. Vincenzo Castiglione, Institute of Life Sciences, Scuola Superiore Sant'Anna, Piazza Martiri della Libertà, 33, 56127 Pisa, Italy. E-mail: vincenzocastiglione93@gmail.com.

REFERENCES

- Gombos Z, Zhang PJ. Glomus tumor. *Arch Pathol Lab Med* 2008;132:1448-52.
- Brouillard P, Ghassibe M, Penington A, et al. Four common glomulin mutations cause two thirds of glomuvenous malformations ("familial glomangiomas"): evidence for a founder effect. *J Med Genet* 2005;42:e13.
- Harrison B, Sammer D. Glomus tumors and neurofibromatosis: a newly recognized association. *Plast Reconstr Surgery Glob Open* 2014;2:e214.
- Folpe AL, Fanburg-Smith JC, Miettinen M, Weiss SW. Atypical and malignant glomus tumors: analysis of 52 cases, with a proposal for the reclassification of glomus tumors. *Am J Surg Pathol* 2001;25:1-12.
- Balisan OP, Radin CPT II, Arias R, Templo F Jr. Malignant glomus tumor of the heart in a 64-year old male presenting with stroke. *Philipp J Pathol* 2018;3:20-3.
- Riesner K, Boecker W. Cardialer Glomustumor, Licht-und elektronenoptische Befunde. *J Cancer Res Clin Oncol* 1975;84:59-66.
- Karapinar K, Kaplan S, Zengin NI, Yuçel E. Glomus tumor of the heart: report of an extreme case. *Chirurgia* 2005;18:125-7.
- Ferrera C, Escribano N, Ortega L, et al. Left ventricular glomangioma. *Int J Cardiol* 2012;160:e38-9.
- Ejaz K, Raza MA, Aleem A, Maroof S, Tahir H. Glomangiosarcoma involving the heart with an unknown primary lesion. *Cureus* 2018;10:1-4.
- Polymerou I, Ojala T, Bonou P, Martelius L, Tzifa A. Successful treatment of cardiac haemangiomas with oral propranolol: a case series of two patients. *Eur Heart J Case Rep* 2019;3.

KEY WORDS cardiac mass, cardiac tumor, glomangioma, glomus tumor

APPENDIX For a supplemental figure and videos, please see the online version of this paper.